

## Acoustic characteristics of a surface-acoustic-wave resonator made of two Bragg reflectors with periodic metallization of GaAs

R. Takasu, Y. Sato, and T. Fujisawa

Department of Physics, Tokyo Institute of Technology.  
2-12-1-H81, Meguro, Tokyo 152-8551, Japan  
Phone: +81-3-5734-2809 E-mail: takasu.r.aa@m.titech.ac.jp

**A surface-acoustic-wave (SAW) resonator, which confines SAW phonons in a small gap between two Bragg reflectors, is attractive for developing acoustic analog of cavity quantum electrodynamics. We have investigated acoustic characteristics of SAW resonators made by patterning a metal film of Cr, Ti, and Au on GaAs. The resonator modes in the acoustic band gap are identified by measuring radio-frequency reflection spectrum of the device and by comparing it with numerical simulations. The obtained parameters will be valuable in designing a high-quality SAW resonator coupled to electronic devices like a double quantum dot.**

### 1. Introduction

Electron-phonon interaction in electronic devices can be utilized attractively by confining phonons at localized electrons embedded in an acoustic resonator [1,2]. A double quantum dot (DQD) in a surface-acoustic wave (SAW) resonator is a promising platform to search for novel cavity quantum electrodynamics. However, in order to prepare the system in the so-called strong coupling regime or ultra-strong coupling regime, smaller phonon resonators are highly desirable [1]. In the case of SAW resonators made of two Bragg reflectors with periodic metallization, acoustic properties of metallized region determine the resonator characteristics. They can be quantified by the material parameters  $F_v$  for velocity change and  $F_r$  for reflection, as defined later. Although these values can be estimated from elastic constants of the bulk materials [3], experimental values for realistic thin metal films are valuable for designing a practical device structure. In contrast to matured SAW materials such as lithium niobate and quartz, acoustic characteristics for GaAs SAW is not fully investigated.

Here we have fabricated SAW resonators by metallizing GaAs surface with three kinds of metals, Cr, Ti, and Au, and experimentally determined  $F_v$  and  $F_r$  for these metals by measuring the reflection spectrum of the devices. We have tested two kinds of resonators; single mode resonators with various gap lengths and multi-mode resonators with a long gap. Both results are consistent to each other and numerical simulations with  $F_v$  and  $F_r$ . However, we find a notable difference between the experimental values and the estimated values from the bulk elastic constants.

### 2. Single and multi-mode SAW resonators

Figure 1(a) shows a schematic design of SAW resonators used in this work. Two Bragg reflectors, each consists of an

interdigital transducer (IDT) with  $N_{\text{IDT}}$  metal fingers and SAW reflectors with  $N_{\text{ref}}$  fingers, are placed symmetrically with a finite gap  $g$  between the inner edges of the metallized regions. The device works for SAWs at around the nominal wavelength  $\lambda_{\text{nom}} = 2a = 20 \mu\text{m}$  and the corresponding frequency  $f_{\text{nom}} \sim 140 \text{ MHz}$  for the period  $a$  of the fingers. The important parameters of the resonator are the velocities in the metallized and free regions,  $v_M$  and  $v_F$ , respectively, and the reflection coefficient  $r$  at the boundary of the two regions. For thin metal layers with the thickness  $h$ , convenient linear dependences,

$$(v_M - v_F)/v_F = F_v h/\lambda_{\text{nom}} \text{ and } r = F_r h/\lambda_{\text{nom}}, \quad (1)$$

can be assumed with the factors  $F_v$  and  $F_r$ . Here, piezoelectric contributions are neglected for GaAs with low piezoelectricity. The objective of this work is experimental determination of these values.

Basically a periodic metal structure with finite  $r$  exhibits a phonon band gap, in which Bragg reflector works, of the width  $\Delta f_{\text{gap}} = (4r/\pi)f_{\text{nom}}$  around the central frequency  $f_c = v_{\text{av}}/\lambda_{\text{nom}}$  with the average velocity  $v_{\text{av}} = 2/(1/v_M + 1/v_F)$  for the metallization ratio being one half. The  $n$ -th resonant frequency  $f_n$  is determined by the interference between the two Bragg reflectors. For simplicity, it can be expressed by an approximate form  $f_n = n(g/v_F + \lambda_{\text{nom}}/rv_{\text{av}})^{-1}$  near  $f_c$ . Therefore, a resonator exhibits a single resonance mode inside the band gap for small  $g$  ( $\ll \lambda_{\text{nom}}/r$ ), and multiple modes for large  $g$ .

The SAW resonators were investigated by measuring RF reflection coefficient  $S_{11}$  at the left IDT in Fig. 1(a). Typical experimental data for some single mode resonators with a Ti layer of  $h = 300 \text{ nm}$  are shown by thick lines in Fig. 1(b) with different  $g$ . A spectrum for a multimode resonator of  $h = 150 \text{ nm}$  is shown in Fig. 1(d). The resonant modes appear as a sharp dips in  $S_{11}$ . These experimental characteristics are compared with numerical simulations with the electromechanical coupling constant  $K^2 = 0.07\%$  for GaAs SAW [3], as shown by thin lines in Fig. 1(b-d). Excellent agreements between the experiment and the simulation are seen by choosing  $r = 0.8\%$  and  $v_M = 0.986v_F$  for Fig. 1(b) and  $r = 0.34\%$  and  $v_M = 0.994v_F$  for Fig. 1(d).

It is instructive to identify the origin of these dips. For a single mode resonator, the resonant frequency changes from the upper end to the lower end of the bandgap by varying  $g$ . This frequency shift with respect to  $g$  is roughly given by  $df_n/dg = (rv_{\text{av}}/av_g)f_n$ . Therefore, one can estimate  $v_{\text{av}}$  and  $r$  from  $f_c$  and  $df_n/dg$ . Other dips at around 144 MHz corresponds to the IDT modes that appear just above the upper end (for  $r$

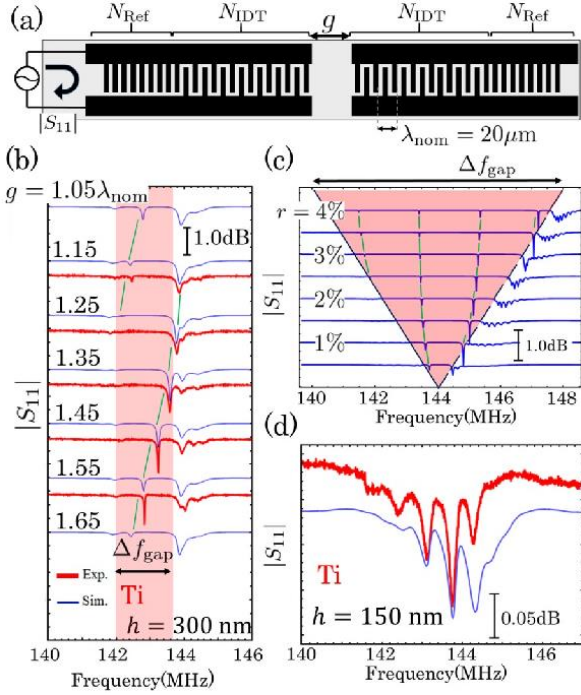


**Fig. 1** (a) Schematic layout of a SAW resonator with a gap  $g$  and the number of fingers,  $N_{\text{IDT}}$  and  $N_{\text{Ref}}$ . (b) Reflection spectrum  $S_{11}(f)$  for single-mode resonators ( $N_{\text{IDT}} = N_{\text{Ref}} = 120$ ). Thick lines represent experimental data with a Ti layer of  $h = 300$  nm, and thin lines represent simulated ones with  $r = 0.8\%$ . The spectral shift of the resonator mode is highlighted by thin lines. The phonon band gap is shown by a colored stripe. (c) Calculated reflection spectra for multi-mode resonators ( $N_{\text{IDT}} = 80$ ,  $N_{\text{Ref}} = 400$ , and  $g = 30 \lambda_{\text{nom}}$ ). (d) Experimental  $S_{11}(f)$  for a long gap  $g = 30 \lambda_{\text{nom}}$  with a Ti layer of  $h = 150$  nm.

$> 0$ ) of the band gap, and these frequencies do not change so much with  $g$ . These IDT modes have nearly standing-wave nature with a strong coupling to the IDT electrodes. Tiny dips at around 142 MHz (the lower end of the bandgap) are attributed to anti-IDT modes weakly coupled to the IDT electrodes. All of these features are seen in both the experiment and the simulation.

Multimode resonators are attractive for their rich structure as seen in Fig. 1(d). As shown in numerical simulations for various  $r$  in Fig. 1(c), the number of resonances increases with  $r$ . This is convenient for estimating the parameters from one device. Comparison with the simulation allows us to identify the resonator and IDT modes and estimate the parameters.

### 3. Comparison between metals

Figures 3(a-c) show typical spectra  $S_{11}$  for short SAW resonators metallized with (a) Cr, (b) Ti, and (c) Au of the same thickness  $h = 300$  nm. The reflection dips associated with the resonator and IDT modes are marked by arrows. As compared to Cr and Ti, the dips with Au are smaller and broader probably due to its grained surface. The estimated phonon band gaps are represented by colored stripes. The estimated parameters for all devices are summarized in Fig. 2(d) for  $r$  and 2(e) for  $f_c$ , from which we have obtained the factors  $F_v$  and  $F_r$  as shown in the Table I.

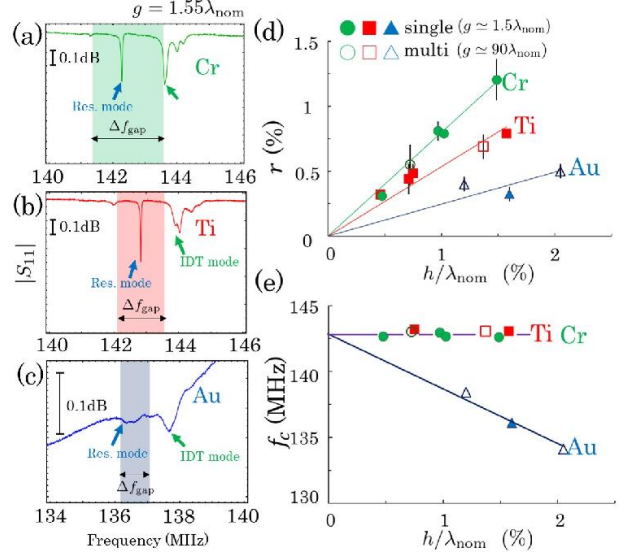


**Fig. 2** (a-c) Reflection spectrum  $S_{11}(f)$  for (a) Cr, (b) Ti, and (c) Au layer ( $h = 300$  nm,  $N_{\text{IDT}} = N_{\text{Ref}} = 120$ , and  $g = 1.55 \lambda_{\text{nom}}$ ). (d and e) The reflection coefficient  $r$  in (d) and the central frequency  $f_c$  in (e) as a function of  $h/\lambda_{\text{nom}}$  for Cr (circles), Ti (squares), and Au (triangles) layers in single- (solid symbols) and multiple- (open symbols) mode resonators. The solid lines are guides to the eye.

**Table I** Elastic parameters,  $F_r$  and  $F_v$ , measured in this work and estimated from bulk material constants.

Elastic parameter	Cr	Ti	Au
$F_r$ measured	1.59	1.07	0.49
estimated from bulk	4.15	1.76	-0.47
$F_v$ measured	$\sim 0$	$\sim 0$	-0.64
estimated from bulk	0.3	0.07	-0.96

These values are compared with the estimated values from bulk properties by using the formula shown in Ref. 3. Although the order of the metals (Cr, Ti, and Au in the descending order of  $F_r$ ) is the same, we see a significant difference between the experimental and bulk values. The difference could be related to the interface and surface effects including oxidation of the thin metal layer.

### 4. Summary

We have investigated acoustic characteristics of SAW resonators made by metallization of GaAs with Cr, Ti, and Au. The experimentally determined  $F_v$  and  $F_r$  will be useful in designing SAW resonators for studying novel electron-phonon interaction.

### Acknowledgements

We thank M. Hashisaka for experimental advice. This work was supported by JSPS KAKENHI (JP26247051 and JP15K13271) and Nanotechnology Platform Program at Tokyo Tech.

### References

- [1] M. J. A. Schuetz et al. Phys. Rev. X 5, 31031 (2015).
- [2] J. C. H. Chen et al., Sci. Rep. 5, 15176 (2015).
- [3] S. Datta, *Surface Acoustic Wave Devices*, Prentice-Hall (1986).